Ionization instability of a Townsend discharge

I. D. Kaganovich, M. A. Fedotov, and L. D. Tsendin

St. Petersburg State Technical University; "Plazma" Scientific-Industrial Consortium, Ryazan'
(Submitted April 18, 1993)
Zh. Tekh. Fiz. **64**, 22–32 (March 1994)

The transition from a Townsend discharge to a normal glow discharge in neon is investigated in the range of pressures from 50 to 200 torr for electrodes (diameter 15 mm) separated by a distance from 1 to 7 mm and currents up to 1 mA. It is shown theoretically and experimentally that at these pressures a Townsend discharge becomes unstable, even for quite low current densities, when the discharge potential falls a few percent below the potential needed to initiate it. The instability leads to the formation of a two-dimensional discharge with a complicated shape. In contrast with a normal discharge, the apparent (visual) size of the column can decrease as the current rises. Strong relaxation oscillations are observed in the transition from a Townsend discharge to a normal discharge at pressures above 100 torr. As the current increases the discharge goes over to the ordinary form, but regimes are also possible in which the total current exhibits small oscillations.

INTRODUCTION

Townsend discharges have been observed for a relatively long time,[1] but almost no studies have been done of filamentation instability in them. At the same time, a Townsend discharge is the simplest type of gas discharge, in which the effect of the self-consistent field is minimal. Hence the study of its stability and of the formation of spatially inhomogeneous two- and three-dimensional structures can shed light on the mechanisms for such phenomena in more complicated systems.

It is well known that instabilities can develop in a Townsend discharge, leading to filamentation at intermediate pressures[2] and to the development of oscillations in the discharge current and voltage.[3] It is found that in the transition from the Townsend to the normal glow form, a discharge can develop complicated two-dimensional shapes accompanied by pronounced oscillations of the discharge current and not included in the Klyarfel'd classification scheme.[4]

The present study was undertaken in order to make a detailed study of the region in which the transition from a Townsend discharge to a normal discharge occurs.

DESCRIPTION OF THE EXPERIMENTAL APPARATUS

The measurement was performed in pure neon in the pressure range 50–200 torr in the device shown in Fig. 1a.

The experimental apparatus (Fig. 1a) was fabricated of molybdenum glass outgassed at a temperature of 400 °C. A mass-spectrometric analysis of the fill gas revealed no impurities. The solid electrodes, fabricated from Al of 99.999% purity, had a diameter of 15 mm, and their faces were within 0.015 radians of being exactly parallel. All measurements were carried out over a time shorter than that required to heat the cathode surface by 2 °C. The anode was shifted simultaneously with a steel weight by means of a permanent magnet made of Co–Sm alloy. A third electrode, exactly the same as the cathode and anode in geometry and composition, was used as a getter to scrub the neon and insure the purity of the gas during the course of the experiments.

When a sawtooth voltage pulse was applied from the generator 5 (Fig. 1b), the potential at the output of the high-voltage generator 4 rose. The discharge current and potential were measured with an xy recorder, the input circuits of which are indicated in the block diagram by the numbers 3–6 respectively. The oscilloscope traces of the discharge current and voltage oscillations were observed by means of a high-frequency dual-trace oscilloscope 1; the discharge spectrum was measured by a recording spectrum analyzer 2.

EXPERIMENTAL RESULTS: TOWNSEND DISCHARGE

Figure 2a shows the typical form of the current–voltage (I–V) characteristic. The I–V characteristic clearly exhibits three regions: the left, corresponding to the Townsend discharge; the right, which completely agrees with the I–V characteristics of a normal discharge; and an intermediate region, which can be regarded as a seminormal discharge.

All I–V characteristics were measured in two directions: first as the current rose from zero to its maximum, and then as it decreased. When this was done the portions corresponding to the Townsend discharge and to the normal glow showed almost no change, but the transition from seminormal to Townsend discharge exhibited considerable hysteresis. In some instances a small amount of hysteresis was observed in the transition from a normal discharge to a seminormal one. Current–voltage characteristics of the same form have been obtained previously.[2,5]

Discharges in the regimes corresponding to the different regions are sharply distinguished from one another. In the Townsend discharge region there is a weak diffuse glow. At very low currents it is concentrated near the anode, since the electron density and the emission are proportional to $\exp\int_0^x \alpha dx$, where α is the Townsend coeffi-

 1063-7842/94/030241-06$10.00

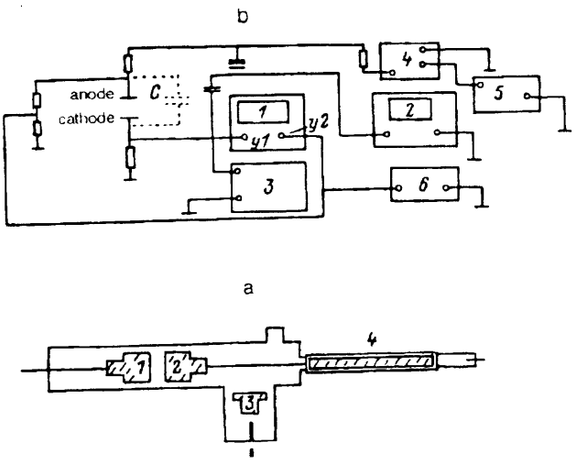

FIG. 1. a: Experimental device: 1) cathode; 2) anode; 3) auxiliary electrode; 4) magnet for shifting the anode. b: Block diagram of the experimental facility: 1) dual-trace oscilloscope; 2) recording analyzer for the signal spectrum; 3) device for detecting the discharge current; 4) high-voltage power supply with analog input; 5) sawtooth wave generator; 6) device for measuring the potential at the anode.

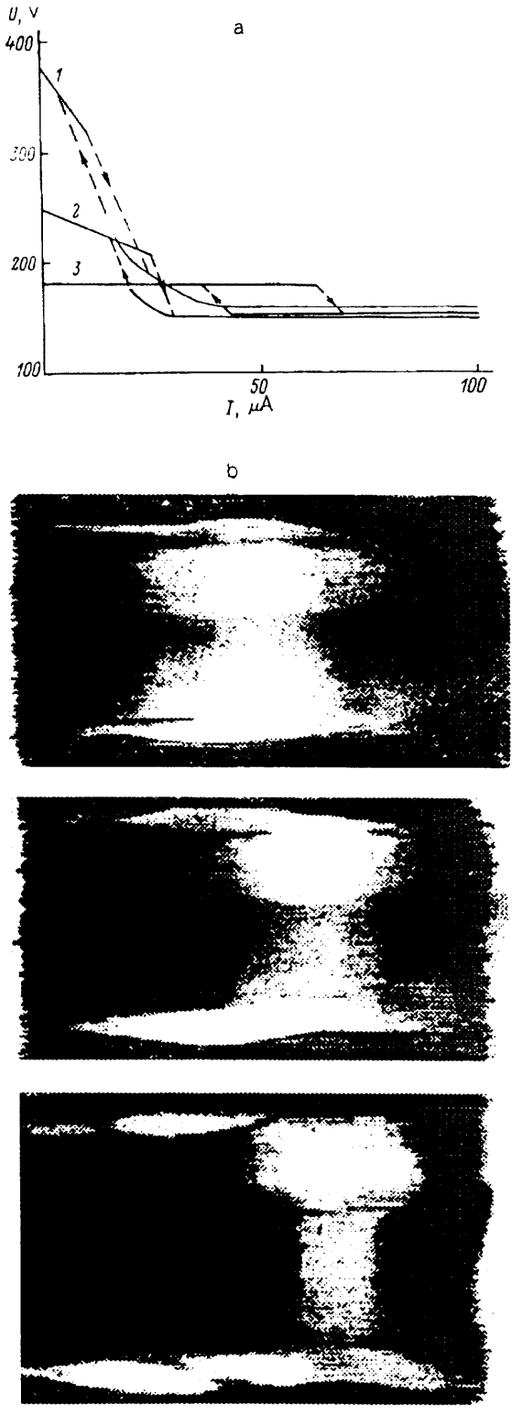

FIG. 2. a: I–V characteristic: $p=50$ torr; $L=1$ (1), 4 (2), and 9 mm (3) b: Form of the two-dimensional discharge for $p=100$ torr, $L=4$ mm; from top to bottom, time-averaged current $I=20$, 30, and 40 μA.

cient, which is largest at the anode. As the current increases, the glow spreads to the cathode surface. This occurs at an ion density such that $\int_0^x \alpha(E)dx$ saturates near the cathode on account of the field distortion due to space charge and the strong dependence of α on the field E at small values of E. The ionization peak shifts from the cathode toward the anode,[6] resulting ultimately in the formation of a cathode sheath.

Striations are observed in the glow region, associated with the relaxation of the electron beam emitted from the cathode toward a uniform distribution in the prescribed field E (Refs. 7 and 8). The separation between striations is such that the voltage drop across a striation is close to the first excitation potential.

When a certain critical current I_1 is reached, the Townsend discharge becomes unstable and the discharge contracts into a filament of diameter 2–4 mm. When this happens a glowing cathode spot is connected to the anode by a cylindrical plasma column. As the current increases, the glow region undergoes a change in appearance and assumes the shape of a kerosene lamp chimney (Fig. 2b), with the narrow part at the anode. In addition to the cathode spot and the plasma column, traces of diffuse emission in the region adjacent to the column are observed during the transition between the Townsend discharge and the normal glow. At currents above some value I_2 the diffuse glow entirely disappears, the area of the spot is drastically reduced, and when the current is increased further a normal glow discharge is observed.

INSTABILITY OF THE TOWNSEND DISCHARGE

At intermediate pressures a Townsend discharge has a gently decreasing current–voltage characteristic. As will be seen below, a drop of even a few percent in the voltage can induce instability in the discharge. Consequently, any small effect that causes the current–voltage characteristic to drop off can induce discharge instability. Mechanisms for this include distortion of the field by the space charge,

gas heating, or the dependence of the electron emissivity γ on the ion energy and hence on the strength of the field at the cathode.[3] The decrease in the discharge voltage is easy to determine, assuming small γ and small nonuniformity of the field.

The equations describing the evolution of the electron density n_e and ion density n_i and the Poisson equation take the form

$$\frac{\partial E}{\partial x}=4\pi e(n_i-n_e),$$

$$\frac{\partial n_e}{\partial t}+\operatorname{div} n_e v_e-D_e\Delta n_e=\alpha(E)v_e n_e,$$

$$\frac{\partial n_i}{\partial t}-\operatorname{div} n_i v_i=\alpha(E)v_e n_e \tag{1}$$

with the boundary conditions $n_i=0$ at $x=L$ (at the anode) and

$$\Gamma_e\equiv n_e v_e=\gamma n_i v_i=\gamma\Gamma_{ik}=\frac{\gamma}{1+\gamma}\frac{j}{e}$$

at $x=0$ (at the cathode); v_e and v_i are the electron and ion drift velocities, Γ_e and Γ_i are the corresponding fluxes, L is the interelectrode gap, D_e is the electron diffusion coefficient, and j is the current density.

Since the distortions in the field are small, we can assume that v_i and v_e are constant and include the variation of the field only in the expression for the Townsend coefficient α. For a steady discharge the ion density profile takes the form

$$n_i=\frac{\Gamma_{ik}(1+\gamma)}{v_i}\left[1-e^{-\int_x^L\alpha dx}\right]. \tag{2}$$

For small currents such that

$$\hat{\alpha}4\pi e n_i L^2\ll v_0, \tag{3}$$

where $\hat{\alpha}=\partial\ln\alpha/\partial\ln E$, and v_0 is the ignition voltage, the variation of α as a function of the field is weak and the second term in square brackets in Eq. (2) can be neglected for $L-x<1/\alpha\ll L$.

Thus, except for a small region near the anode the ion density $n_i(x)$ can be taken constant, and the electron density is small in comparison with n_i. The decrease in the potential is determined from the condition for a steady discharge,

$$\int_0^L\alpha dx=\ln\left(\frac{1}{\gamma}+1\right). \tag{4}$$

Substituting a linear profile for the field

$$E=\frac{V_0}{L}+\frac{\delta V}{L}-4\pi e n_i\left(x-\frac{L}{2}\right),$$

we find the decrease in the discharge voltage with respect to the ignition voltage[9]

$$\frac{\delta V}{V_0}=-\frac{\frac{2L}{3}\frac{\partial^2\alpha}{\partial E^2}(\pi e n L)^2+\frac{\partial\ln\gamma}{\partial E}2\pi e n L}{\frac{\partial\alpha}{\partial E}V_0}-\frac{\overline{\delta T}}{T}. \tag{5}$$

where $\overline{\delta T}$ is the gas heating averaged over the discharge gap and T is the electron temperature.

The first term corresponds to the effect of the field variation and gives rise to a parabolic current dependence with $\delta V\ll V_0$; the second term takes into account the increase of γ due to the rise in the field at the cathode; the third term describes the average heating of the gas. The second and third terms yield a linearly decreasing I–V characteristic, which can give rise to an instability at low current densities.

Let us analyze the stability of the system of equations (1), restricting ourselves to the two-dimensional case. We will look for a solution for the perturbation in the form $\Gamma_e(y,x)=\Gamma_e(x)\sin kye^{\Omega t}$. Since the discharge evolution occurs on the ion time scales, we can disregard the time derivatives in the electron equation and find [for $\alpha=\text{const}=\alpha(V/L)$] an expression for the perturbation of the electron flux in the form

$$\Gamma_e(x)=\Gamma_e(0)e^{(\alpha-(D_e/v_e)k^2)x}. \tag{6}$$

Integrating the ion equation across the discharge gap and expressing the ionization in terms of the electron flux, we find

$$\frac{\partial}{\partial t}\int n_i dx=\Gamma_e(L)-\Gamma_e(0)-\Gamma_i(0)-D_e\int\Delta n_e dx. \tag{7}$$

Near the boundary of instability its growth time is much longer than the ion time scale L/v_i, so the ion density profile can be treated as quasistationary and [when condition (3) holds] uniform. Using (6) and (7), we find an expression for the damping rate Ω_d to within terms of order $(\ln\gamma)^{-1}$:

$$\Omega_d=-\frac{D_e}{v_e}v_i k^2=-D_{ef}k^2. \tag{8}$$

At first glance it appears paradoxical that electron diffusion gives a small damping rate, on the order of the inverse ion diffusion time. The reason for this is that if the electron multiplication is limited by ion–electron emission from the cathode, then in the time L/v_e required to pass from the cathode to the anode the electron avalanche spreads over a distance

$$\Delta r\sim\left(\frac{D_e L}{v_e}\right)^{1/2} \tag{9}$$

where D_e is the electron diffusion coefficient.

The spreading process repeats itself over the time L/v_i required for the ions produced in the avalanche to drift to the cathode. As a result, after a time t the irregularity has diffused over a distance given by $r^2=(\Delta r)^2\cdot v_i t/L$, since the variances add in a diffusion process. The effective diffusion coefficient

$$D_{ef}=r^2/t=\frac{v_i D_e}{v_e} \tag{10}$$

is equal to the ambipolar diffusivity.

Any process that increases the quantity $\int_0^L \alpha dx$ at a fixed potential V contributes to the instability growth rate. The formula for the growth rate is obtained in analogy with (8):

$$\Omega_i=v_i\frac{\partial\alpha}{\partial E}\frac{\partial V}{\partial n}\frac{n}{V}\frac{\gamma_i+\gamma_\Phi}{\gamma_1+\gamma_\Phi v_i/v_e}f(kL), \tag{11}$$

where $\partial V/\partial n$ is given by Eq. (5) and the function $f(z)$ takes into account bending of the field lines by the y-dependent space charge.

If the ion density profile is proportional to $\cos(ky)$, then the solution of the Poisson equation between plane-parallel conducting plates takes the form

$$\varphi=\left(-\frac{4\pi e n_0}{k^2}+A\cosh kx+B\sinh kx\right)\cos ky,$$

$$\varphi(x=0)=0;\quad \varphi(x=L)=V.$$

The quantity $\int\alpha[E(\xi)]d\xi$, taken along a field line between the electrodes, differs from the value $\int_0^L\alpha[E(x)]dx$ calculated without including two-dimensional effects (for $k=0$) by a factor

$$f(kL)=\frac{3}{(kL)^2}\left[1-\frac{\tanh kL}{kL}\right].$$

The lengthening of the field lines at a fixed potential drop between the anode and cathode corresponds to a decrease in the average field compared to V/L and reduces the integral $\int_0^L\alpha dx$, and hence the growth rate. For fluctuations with $kL\ll 1$ we have $f\to 1$ and the bending can be disregarded.

If we compare the expressions for the damping and growth rates we find that the instability occurs for small values of $\delta V/V_0$:

$$\delta V\approx\frac{\partial V}{\partial n_i}\approx\frac{T_e(kL)^2\ln(1/\gamma)}{ef(kL)\hat{\alpha}}, \tag{12}$$

where $T_e=eD_e\cdot E/v_e$ is the effective electrode temperature and k is the minimum wave number determined by the transverse dimension of the electrodes.

For large values of pL, when the quantity α depends strongly on E, this instability should grow rapidly, since the Landau constant, which is proportional to $\partial^2\alpha/\partial E^2$ is positive.[10] Consequently, the transition to and from a two-dimensional discharge takes place with considerable hysteresis (Fig. 2a). The transition currents depend sensitively on the way the change in the discharge current is controlled. With fast automatic control (when the I–V characteristic is measured in 10 s) the transition currents are larger by 10–30% than when the variation is done by hand (over a time of order 10 min).

The value of the potential at which stability is lost agrees well with the values given by Eq. (12). This indicates that the main stabilizing mechanism is transverse ambipolar diffusion. For example, under conditions corresponding to Fig. 2a (transition current $I_c=22.5\ \mu$A, $p=50$ torr, $L=4$ mm), the right-hand side of (12) yields $\delta V=50$ V, whereas the experimental value is $\delta V=32$ V. In the calculations we used the following values of the parameters: $T_e=D_e(E_0)/v_e(E_0)=6$ eV (Ref. 11) and $\ln(1/\gamma+1)=\alpha(E_0)L=1.2$, $\hat{\alpha}=2$, corresponding to the experimentally observed field $E_0=V_0/L$. Under these conditions the calculation of the growth rate according to (5) implies that the thermal instability mechanism makes a small contribution (for $I=I_c$ the gas heated up less than 0.1 °C), while including the field distortion due to the ion space charge (5), (12) yields a value $I_c=20\ \mu$A. It should be kept in mind, however, that expression (5) for the I–V characteristic under these conditions is inapplicable, strictly speaking, since the deformation of the field in the x direction even for $I\leqslant I_c$ is not small. This is corroborated by the fact that at low currents a maximum of the emission intensity is observed near the anode, in accordance with (3), while for $I\sim 10\ \mu$A a transition occurs to a regime in which the emission intensity is nearly uniform. Moreover, in deriving (5) we assumed that the ion density does not depend on x. These same factors are probably responsible for the fact that the I–V characteristic of the discharge for $I\leqslant I_c$ deviates from the quadratic dependence $\delta V\sim I^2$ suggested by the simple formula (5).

In addition to filamentation, instabilities can develop in the discharge that give rise to oscillations of the total current and voltage of the discharge.[3] For this to happen it is necessary that one of the conditions

$$R<R_d,\quad \Omega_i>1/(RC)$$

be satisfied, where R,C are the resistance and capacitance of the system consisting of the discharge and the external circuit; R_d is the differential resistance of the discharge.

The oscillations in the discharge begin to grow before the filamentation if

$$\frac{1}{RC}<\Omega_d, \tag{13}$$

where Ω_d is given by Eq. (8).

In our experiments, when the quantity RC exceeded some threshold value $(RC)_k$ the current of the transition to the two-dimensional discharge state began to decrease as a function of RC, which is in close accord with the criterion (13). For example, for $p=50$ torr, $d=9$ mm the experimental value was $(RC)_k=1.4\cdot 10^{-3}$ s, while the damping rate was $\Omega_d=1.6\cdot 10^3\ \text{s}^{-1}$.

DISCHARGE STATES AFTER THE DEVELOPMENT OF THE INSTABILITY

When RC is sufficiently small, no oscillations develop anywhere in the transition region from the Townsend discharge to the normal discharge.[12] When instability develops, the discharge changes discontinuously into the two-dimensional steady state with a potential greater than the normal one and current density considerably less than normal (the I–V characteristic in Fig. 2a). As the current

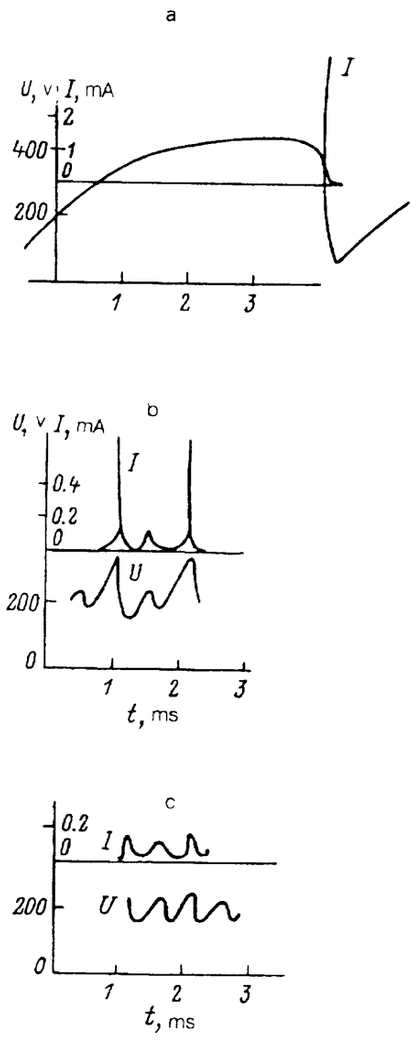

FIG. 3. Current and voltage oscillations in the discharge: $p=50$ torr, $C=48$ pF. $R_d=14$ MΩ, $L=9$ mm; I, μA: a) 8.64; b) 45; c) 48. a: Relaxation oscillations; b: period-doubling bifurcation; c: frequency-doubling bifurcation.

increases, the diameter of the filament initially remains constant ~3 mm and then increases following the normal current density law.

The discharge assumes a considerably more complicated shape if intense oscillations develop in parallel with the contraction in the discharge. In this case, after the instability has developed the observed diameter of the discharge can decrease as a function of current, and the discharge shape changes from cylindrical to the shape of a kerosene lamp chimney with the narrow part at the anode (Fig. 3). At low currents, close to the instability boundary, strong relaxation oscillations develop (periodically repeated breakdown).

The current pulse length is short (about 1–3 μs, independent of the current), and the current has a large amplitude (several mA), considerably greater than the average discharge current in this regime (20–100 μA). The interval T between pulses is a few hundred μs. The voltage across the discharge has a shape close to sawtoothed. The pulse amplitude changes little when the current varies.

Prior to a current pulse the voltage across the discharge gap increases from some value V_2 to the breakdown voltage V_1. The duration of this stage is determined by the RC constant of the circuit and the emf of the power supply.[12] Then the charge $Q=C(V_1-V_2)$ accumulated on the electrodes is released through the discharge. The characteristic time for this stage is evidently determined by the ion time $\tau\sim v_i/L$. The voltage falls to the value V_2, which is independent of the current and depends very weakly on the circuit parameters (RC) and the discharge parameters (p,L). In our experiments it had a value $V_2\sim 100$ V. The difference between it and the potential corresponding to the normal current density ($V_n=150$ V) is probably related to inertial effects.

The amplitude of the current pulse

$$A\sim\frac{C(V_1-V_2)}{\tau}$$

depends weakly on the average current and increases as a function of pL and C. For example, when the capacitance was increased from 50 to 100 pF ($p=50$ torr, $L=8$ mm), we found that A increased from 4.4 to 9 mA, and when the gap was decreased from 9 to 4 mm it decreased to 1.5 mA. As the average current $\bar{I}\sim A\tau/T$ increases, the period decreases in inverse proportion to the average current, since the quantity $A\tau=C(V_2-V_1)$ does not change.

When T decreases to the critical value T_c (e.g., $T_c\sim 0.8$ ms for $p=50$ torr and $L=9$ mm) a period-doubling bifurcation occurs.[12] T_c depends weakly on the parameters R and C of the external circuit. When bifurcation occurs the pulse amplitude abruptly decreases (by a factor of 4–8), the maximum potential V_1 of the pulses decreases and becomes less than the ignition voltage, and the minimum potential V_2 increases weakly. The pulse shape is shown in Fig. 3b. When the average current is increased further the shape of the voltage pulses does not change, but their period decreases. In this case a current which is small but comparable with the mean current flows through the discharge between current pulses. When the period is reduced to T_c, frequency doubling occurs, reversing the bifurcation. The current oscillations undergo a discontinuous change in shape. Instead of relatively widely separated pulses, oscillations with current modulation of order 10–50% set in (Fig. 3c). The period and amplitude of the current and voltage oscillations vary in a complicated manner when the discharge current increases: modes with incommensurate frequencies arise and interact (the sum frequencies are observed), and period-doubling bifurcation occurs. The mode frequencies change from 8 to 15 kHz, with the first three harmonics of each oscillation mode being observed, as a rule. We observed discontinuities in the percent modulation of the discharge current, with no change in the average current, the voltage across the discharge, or the spot diameter. As the mean current increases, the oscillation amplitude can change nonmono-

tonically, but at sufficiently large currents (50–100 μA) the discharge goes over to a normal glow discharge without oscillations.

In addition to oscillations and contraction in the transverse direction, in the transition regime we observed striations in the cathode region. We saw 3–4 spatial periods with a length of about 1 mm.

CONCLUSION

In this work we have shown that as pL increases, a Townsend discharge becomes unstable at even lower values of the current. Depending on the parameters, the onset of instability can give rise to a spatially nonuniform steady form of discharge or to an oscillatory regime accompanied by relaxation oscillations or nearly sinusoidal oscillations. In contrast to a normal glow discharge, the diameter of such a discharge can decrease as a function of the current.

[1] R. Seeliger and J. Schnehel, Phys. Z. **26**, 471 (1925).

[2] L. A. Sena and I. R. Ryazantseva, Zh. Tekh. Fiz. **48**, 1643 (1978) [Sov. Phys. Tech. Phys. **23**, 930 (1978)].

[3] V. N. Melekhin and N. Yu. Naumov, Zh. Tekh. Fiz. **54**, 1521 (1984) [Sov. Phys. Tech. Phys. **29**, 888 (1984)].

[4] V. N. Klyarfel'd, L. G. Guseva, and A. S. Pokrovskaya, Zh. Tekh. Fiz. **36**, 704 (1966) [Sov. Phys. Tech. Phys. **11**, 520 (1966)].

[5] Yu. A. Iorish and V. D. Podkolvin, Zh. Tekh. Fiz. **42**, 536 (1972) [Sov. Phys. Tech. Phys. **17**, 424 (1972)].

[6] V. I. Kolobov and L. D. Tsendin, Zh. Tekh. Fiz. **59** (11), 22 (1989) [Sov. Phys. Tech. Phys. **34**, 1239 (1989)].

[7] L. D. Tsendin, Fiz. Plazmy **8**, 169 (1982) [Sov. J. Plasma Phys. **8**, 96 (1982)]; Fiz. Plazmy **8**, 400 (1982) [Sov. J. Plasma Phys. **8**, 229 (1982)].

[8] K. N. Ul'yanov and V. V. Chulkov, Teplofiz. Vys. Temp. **26**, 843 (1988).

[9] A. H. von Engel and M. Stenbeck, *Physics and Technology of Electric Discharge in Gases* [Russian translation], Vol. 2, ONTI, Moscow-Leningrad (1936).

[10] L. D. Landau and E. M. Lifshitz, *Fluid Mechanics*, Pergamon Press, Oxford (1987).

[11] Yu. P. Raizer, *Gas-Discharge Physics*, Springer, New York (1991).

[12] V. N. Melekhin, N. Yu. Naumov, and N. P. Tkachenko, Zh. Tekh. Fiz. **57**, 454 (1987) [Sov. Phys. Tech. Phys. **32**, 274 (1987)].

Translated by David L. Book